Int. J. Solids Structures Vol. 22, No. 11, pp. 1201–1211, 1986
Printed in Great Britain.

0020-7683/86 $3.00+.00
Pergamon Journals Ltd.

FINITE ELEMENT FORMULATION FOR TRANSIENT PORE PRESSURE DISSIPATION: A VARIATIONAL APPROACH

RONALDO I. BORJA
Department of Civil Engineering, University of the Philippines, Quezon City, Philippines

(*Received* 7 *September* 1984; *in revised form* 25 *July* 1985)

Abstract—A finite element formulation for solving general three-dimensional consolidation problems using variational concepts is presented. The formulation involves coupled displacement and pore pressure fields and has been numerically implemented to analyze boundary value problems of axisymmetric (torsionless) and plane strain configurations. Three numerical examples are discussed.

1. INTRODUCTION

The behavior of soils is governed by the difference between the total stresses acting on the soil mass and the pore pressures. In most practical field cases it is necessary to describe the *effective stress field* to characterize the strength and deformation properties of the soil. Although the no-flow (undrained) and the free-flow (drained) conditions can be analyzed using a single-phase continuum formulation, consideration of the two-phase soil–water relationship in a saturated soil medium is essential in characterizing the soil behavior during the transient period of excess pore pressure dissipation.

Derivations of the governing equations coupling the displacement and pore pressure fields can be presented either by direct application of the principle of virtual work, minimization of the total potential energy, application of the principle of stationary potential, or by a variational formulation. It is the objective of this paper to present a finite element formulation for analyzing consolidation or diffusion type of problems using variational concepts, and illustrate how such formulation can be implemented numerically in the solution of initial boundary value problems.

2. FORMULATION

Consider a soil continuum in domain Ω and bounded by surface Γ. Part of its surface Γ_{g_i} is subjected to a prescribed displacement function g_i, while the remainder of its surface Γ_{h_i} is subjected to a traction h_i. The same total surface Γ may also be divided into a portion Γ_r subjected to a prescribed pore pressure function r, and the remainder Γ_s under an input hydraulic flux of s. In symbolic form, assume that the following set relations hold (see Fig. 1):

$$\left.\begin{aligned}\Gamma &= \overline{\Gamma_{g_i} \cup \Gamma_{h_i}} = \overline{\Gamma_r \cup \Gamma_s} \\ \varnothing &= \Gamma_{g_i} \cap \Gamma_{h_i} = \Gamma_r \cap \Gamma_s\end{aligned}\right\}, \tag{1}$$

for $i = 1, \ldots, n_{sd}$, where n_{sd} = number of spatial dimensions, $\varnothing$ = null set, the symbols $\cup$ and $\cap$ represent set *union* and *intersection*, respectively, and the overlines denote a closure.

2.1. *Strong form*

The strong form (S), or the classical statement of the model problem is presented mathematically in rate form as follows (summation implied on repeated subscripts):

Given f_i, g_i, h_i, r and s, find the functions u_i and ρ such that

$$\dot{\sigma}_{ij,j} + \dot{f}_i = 0 \qquad \text{in} \qquad \Omega \text{ (equilibrium)}, \tag{2a}$$

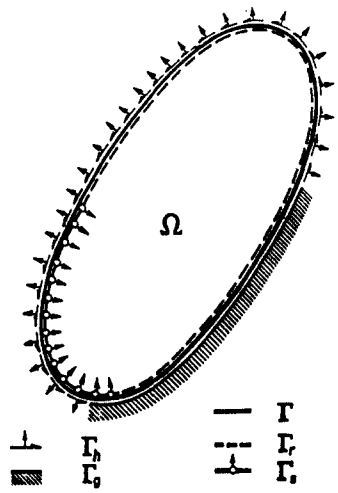

Fig. 1. Problem domain and boundaries.

$$\dot{u}_{i,i} - \dot{\varepsilon}_v = 0 \quad \text{in} \quad \Omega \text{ (continuity)}, \tag{2b}$$

$$\dot{u}_i = \dot{g}_i \quad \text{on} \quad \Gamma_{g_i}, \tag{3a}$$

$$\dot{\sigma}_{ij} n_j = \dot{h}_i \quad \text{on} \quad \Gamma_{h_i}, \tag{3b}$$

$$\dot{\rho} = \dot{r} \quad \text{on} \quad \Gamma_r, \tag{4a}$$

$$\dot{u}_i n_i = s \quad \text{on} \quad \Gamma_s, \tag{4b}$$

where

u_i = ith (Cartesian) component of the displacement field function **u**,
ρ = pore pressure field function,
σ_{ij} = (i,j) component of the symmetric (Cauchy) effective stress tensor $\boldsymbol{\sigma}$, compression positive,
f_i = ith component of the effective body force **f**,
ε_v = volumetric strain, compression positive,
g_i = ith component of the prescribed displacement **g**,
h_i = ith component of the prescribed traction **h**,
r = prescribed pore pressure function,
s = prescribed velocity flux,
n_i = direction cosine of the angle between the (Cartesian) axis i and the surface normal.

Equations (2a) and (2b) are quasi-static rate equations involving effective stresses in a fully saturated soil mass. Consequently, a two-phase water–soil structure is implied. Since water is relatively incompressible compared with the soil skeleton, (2b) states that the rate of volume change equals the rate at which water is squeezed out of the soil mass (see Biot[2]).

2.2. *Weak form*

The weak form (W) or the *variational counterpart* of (S) involves the determination of functions u_i and ρ and the satisfaction of both the differential equations (2a, b) and the boundary conditions (3) and (4) on the basis of weighted averages.

As a prelude to the statement of (W), consider a set of *trial solutions*

$$\begin{aligned} \Upsilon_i &= \{u_i | u_i \in H^1, \quad \dot{u}_i = \dot{g}_i \text{ on } \Gamma_{g_i}\}, \\ \Phi &= \{\rho | \rho \in H^1, \quad \dot{\rho} = \dot{r} \text{ on } \Gamma_r\}, \end{aligned} \tag{5}$$

and a set of *weighting* functions

$$\Theta_i = \{w_i | w_i \in H^1, \quad \dot{u}_i = 0 \text{ on } \Gamma_{g_i}\},$$
$$\Psi = \{q | q \in H^1, \quad \dot{q} = 0 \text{ on } \Gamma_r\}, \tag{6}$$

where H^1 is a set of functions with square-integrable first derivatives,† and w_i and q are any possible "virtual displacements" and "virtual pressures", respectively, in the context of a virtual work formulation. The set symbol $\in$ means "belongs in" or "is an element of".

To develop the weak form of (S), (2a, b) are rewritten, thus:

$$\int_\Omega w_i \cdot (\dot{\sigma}_{ij,j} + \dot{f}_i)\, d\Omega + \int_\Omega q \cdot (\dot{u}_{i,i} - \dot{\varepsilon}_v)\, d\Omega = 0, \tag{7a}$$

or,

$$\int_\Omega w_i \dot{\sigma}_{ij,j}\, d\Omega + \int_\Omega w_i \dot{f}_i\, d\Omega + \int_\Omega q \dot{u}_{i,i}\, d\Omega - \int_\Omega q \dot{\varepsilon}_v\, d\Omega = 0. \tag{7b}$$

Equation (7a) can be verified by observing that the quantities inside the parentheses are zero point-wise.

Using the *divergence theorem* and integrating by parts,

$$\int_\Omega w_i \dot{\sigma}_{ij,j}\, d\Omega = -\int_\Omega w_{i,j} \dot{\sigma}_{ij}\, d\Omega + \int_\Gamma w_i \dot{\sigma}_{ij} n_j\, d\Gamma$$
$$= -\int_\Omega w_{(i,j)} \cdot (c_{ijkl} \dot{\varepsilon}_{kl} - \dot{\sigma}^0_{ij})\, d\Omega + \sum_{n=1}^{n_{sd}} \left(\int_{\Gamma_{h_n}} w_i \dot{h}_i\, d\Gamma_{h_n} \right), \tag{8a}$$

where $w_{(i,j)}$ is the symmetric part of the tensor gradient $w_{i,j}$, while $\dot{\sigma}_{ij} n_j = \dot{h}_i$ from traction boundary condition (3b);

$$\int_\Omega q \dot{u}_{i,i}\, d\Omega = -\int_\Omega q_{,i} \dot{u}_i\, d\Omega + \int_\Gamma q \dot{u}_i n_i\, d\Gamma$$
$$= -\int_\Omega q_{,i} \frac{-k_{ij}}{\gamma_w} \rho_j\, d\Omega + \int_{\Gamma_s} qs\, d\Gamma_s, \tag{8b}$$

upon substitution of $\dot{u}_i n_i = s$ from flow velocity boundary condition (4b).

Equation (8a) assumes a general constitutive equation of the form

$$\dot{\sigma}_{ij} = c_{ijkl} \dot{\varepsilon}_{kl} - \dot{\sigma}^0_{ij}, \tag{9}$$

in which c_{ijkl} is the rank-four material stress-strain tensor and $\dot{\sigma}^0_{ij}$ is the stress relaxation rate which arises due to temperature changes (e.g. cf. (9) with Duhamel–Neumann's generalized form of Hooke's law in thermoelasticity[8, 11]) and/or time-dependent (creep) effects[4, 5]. Equation (8b) is obtained using *Darcy's law* for transient pore pressure dissipation given by

$$\dot{u}_i = -\frac{k_{ij}}{\gamma_w} \rho_j, \tag{10}$$

where γ_w = unit weight of water and $k_{ij} = (i, j)$ component of the permeability tensor **k** (the negative sign implies that the flow goes in the direction of decreasing gradient).

† In general H^n is a set of functions smooth enough to possess square-integrable nth derivatives.

Substituting (8a), (8b) and $\dot{\varepsilon}_v \leftarrow \dot{u}_{i,i}$ in (7b), the statement of the weak form (W) is obtained as follows:

Given f_i, g_i, h_i, r and s as in (S), find $u_i \in \Upsilon_i$ and $\rho \in \Phi$ such that for all $w_i \in \Theta_i$ and $q \in \Psi$,

$$\int_\Omega w_{(i,j)} c_{ijkl} \dot{u}_{(k,l)}\, d\Omega + \int_\Omega w_{i,i} \dot{\rho}\, d\Omega - \int_\Omega q_{,i} \frac{k_{ij}}{\gamma_w} \rho_{,j}\, d\Omega + \int_\Omega q \dot{u}_{i,i}\, d\Omega$$

$$= \int_\Omega w_i \dot{f}_i\, d\Omega + \int_\Omega w_{i,j} \dot{\sigma}^0_{ij}\, d\Omega + \int_{\Gamma_s} qs\, d\Gamma_s + \sum_{n=1}^{n_{sd}} \left(\int_{\Gamma_{h_n}} w_i \dot{h}_i\, d\Gamma_{h_n} \right), \quad (11)$$

where $w_{(i,j)}$ and $\dot{u}_{(k,l)}$ are the symmetric parts of the tensor gradients $w_{i,j}$ and $\dot{u}_{k,l}$, respectively.

Equations (3a) and (4a) are the *essential* boundary conditions repeated explicitly in (5) of the weak form, while (3b) and (4b) are the *natural* boundary conditions which implicitly develop in (11) out of a variational procedure.

In abstract form, (11) is rewritten thus:

$$\mathbf{A}(\mathbf{w}, \dot{\mathbf{u}}) + (\operatorname{div} \mathbf{w}, \dot{p}) - \bar{\mathbf{A}}(q, \rho) + (q, \operatorname{div} \dot{\mathbf{u}}) = (\mathbf{w}, \dot{\mathbf{f}}) + (\partial \mathbf{w}, \dot{\boldsymbol{\sigma}}^0) + (q, s)_\Gamma + (\mathbf{w}, \dot{\mathbf{h}})_\Gamma, \quad (12)$$

where $\mathbf{A}(\cdot, \cdot)$ and $\bar{\mathbf{A}}(\cdot, \cdot)$ are *symmetric bilinear* operators defined by

$$\mathbf{A}(\mathbf{w}, \dot{\mathbf{u}}) = \int_\Omega w_{(i,j)} c_{ijkl} \dot{u}_{(k,l)}\, d\Omega, \quad (13a)$$

$$\bar{\mathbf{A}}(q, p) = \int_\Omega q_{,i} \frac{k_{ij}}{\gamma_w} \rho_{,j}\, d\Omega, \quad (13b)$$

and $(\bigcirc, \bullet)$ is an operator defined by

$$(\bigcirc, \bullet) = \int_\Omega (\bigcirc \bullet)\, d\Omega, \quad (13c)$$

$$(\bigcirc, \bullet)_\Gamma = \int_\Gamma (\bigcirc \bullet)\, d\Gamma. \quad (13d)$$

The weak statement (11) of the model problem parallels that of physical modeling in which stress and strain measurements are obtained on the basis of their average values over a finite region, and not at any single point as suggested by the point-wise satisfaction of (2a, b)[1].

2.3. *Galerkin approximations*

The Galerkin formulation provides the *link* between the weak form (9) and its finite element counterpart by introducing the following approximations:

Let Υ^h, Θ^h, Φ^h and Ψ^h be the *finite dimensional approximations* of Υ, Θ, Φ and Ψ, respectively; i.e. $\Upsilon^h \subset \Upsilon$, $\Theta^h \subset \Theta$, $\Phi^h \subset \Phi$ and $\Psi^h \subset \Psi$, where the symbol $\subset$ means "is a subset of", and the superscript h suggests that these approximations are associated with the discretization of domain Ω into a mesh of subdomains Ω^e.

The Galerkin form (G) of the model problem is stated as follows:

Given $\mathbf{f}$, $\mathbf{g}$, $\mathbf{h}$, r and s as in (S), find

$$\begin{aligned} \mathbf{u}^h &= \mathbf{v}^h + \mathbf{g}^h \in \Upsilon^h, \\ \rho^h &= \varrho^h + r^h \in \Phi^h, \end{aligned} \quad (14)$$

such that for all $\mathbf{w}^h \in \Theta^h$ and $q^h \in \Psi^h$,

$$\mathbf{A}(\mathbf{w}^h, \dot{\mathbf{v}}^h) + (\operatorname{div} \mathbf{w}^h, \dot{\varrho}^h) - \bar{\mathbf{A}}(q^h, \varrho^h) + (q^h, \operatorname{div} \dot{\mathbf{v}}^h)$$
$$= (\mathbf{w}^h, \dot{\mathbf{f}}) + (\partial \mathbf{w}^h, \dot{\boldsymbol{\sigma}}^0) + (q^h, s)_\Gamma + (\mathbf{w}^h, \dot{\mathbf{h}})_\Gamma$$
$$- [\mathbf{A}(\mathbf{w}^h, \dot{\mathbf{g}}^h) + (\operatorname{div} \mathbf{w}^h, \dot{r}^h) - \bar{\mathbf{A}}(q^h, r^h) + (q^h, \operatorname{div} \dot{\mathbf{g}}^h)], \quad (15)$$

where $\mathbf{v}^h \in \Theta^h$ and $\varrho^h \in \Psi^h$.

As an illustration, note that since $\mathbf{v}^h \in \Theta^h \subset \Theta$ and $\varrho^h \in \Psi^h \subset \Psi$, $v_i^h = 0$ on Γ_{g_i} and $\dot{\varrho}^h = 0$ on Γ_r because of (6). Hence, $\dot{u}_i^h = 0 + \dot{g}_i^h = \dot{g}_i^h$ on Γ_{g_i} and $\dot{p}^h = 0 + \dot{r}^h = \dot{r}^h$ on Γ_r, satisfying (14).

2.4. *Matrix form*

Introducing interpolatory expansions for $\mathbf{v}^h$ and ϱ^h and using parallel interpolations for $\mathbf{w}^h$ and q^h,

$$\mathbf{v}^h(\mathbf{x}) = \sum_{a \in \eta - \eta_g} N_a(\mathbf{x}) \mathbf{d}_a, \quad (16a)$$

$$\mathbf{w}^h(\mathbf{x}) = \sum_{a \in \eta - \eta_g} N_a(\mathbf{x}) \bar{\mathbf{w}}_a, \quad (16b)$$

$$\varrho^h(\mathbf{x}) = \sum_{b \in \varsigma - \varsigma_r} \hat{N}_b(\mathbf{x}) p_b, \quad (17a)$$

$$q^h(\mathbf{x}) = \sum_{b \in \varsigma - \varsigma_r} \hat{N}_b(\mathbf{x}) \bar{q}_b, \quad (17b)$$

where N_a are the *displacement shape functions* associated with displacement node a and $\hat{N}_b$ are the *pressure shape functions* associated with pressure node b; $\mathbf{d}_a$ is the nodal displacement vector with elements $\{d_1, \ldots, d_{n_{sd}}\}_a$ at a, p_b is the nodal pressure at b; $(\eta - \eta_g)$ and $(\varsigma - \varsigma_r)$ are the node numbers at which the displacements and pore pressures, respectively, are unknown; $\bar{\mathbf{w}}_a$ and $\bar{q}_b$ are any arbitrary non-zero counterparts of $\mathbf{d}_a$ and p_b.

The arbitrariness of $\bar{\mathbf{w}}_a$ and $\bar{q}_b$ leads to the matrix form (M) of the Galerkin equation, written in segregated **d**–**p** form as

$$\mathbf{K}\dot{\mathbf{d}} + \mathbf{G}\dot{\mathbf{p}} = \dot{\mathbf{F}}, \quad (18a)$$

$$\mathbf{G}^T\mathbf{d} + \mathbf{M}\mathbf{p} = \dot{\mathbf{H}}, \quad (18b)$$

where the global arrays **K**, **G**, $\mathbf{G}^T$, **M**, $\dot{\mathbf{F}}$ and $\dot{\mathbf{H}}$ which emanate from (15) are given in Table 1.

To express these global arrays explicitly on the element level, the (symmetric) stress and strain tensors are vectorized in the order

$$\boldsymbol{\sigma} = [\sigma_{11}, \sigma_{22}, \sigma_{33}, \sigma_{12}, \sigma_{23}, \sigma_{13}]^T \quad (19a)$$

Table 1.

GLOBAL ARRAY	TERMS IN GALERKIN EQUATION
K	$\mathbf{A}(\mathbf{w}^h, \dot{\mathbf{v}}^h)$
G	$(\operatorname{div} \mathbf{w}^h, \dot{\varrho}^h)$
$\mathbf{G}^T$	$(q^h, \operatorname{div} \dot{\mathbf{v}}^h)$
M	$-\bar{\mathbf{A}}(q^h, \varrho^h)$
$\dot{\mathbf{F}}$	$(\mathbf{w}^h, \dot{\mathbf{f}}) + (\partial \mathbf{w}^h, \dot{\boldsymbol{\sigma}}^0) + (\mathbf{w}^h, \dot{\mathbf{h}})_\Gamma$ $- [\mathbf{A}(\mathbf{w}^h, \dot{\mathbf{g}}^h) + (\operatorname{div} \mathbf{w}^h, \dot{r}^h)]$
$\dot{\mathbf{H}}$	$(q^h, s)_\Gamma - [(q^h, \operatorname{div} \dot{\mathbf{g}}^h) - \bar{\mathbf{A}}(q^h, r^h)]$

$$\boldsymbol{\varepsilon} = [\varepsilon_{11}, \varepsilon_{22}, \varepsilon_{33}, 2\varepsilon_{12}, 2\varepsilon_{23}, 2\varepsilon_{13}]^{\mathrm{T}}, \tag{19b}$$

respectively, while the rank-four stress-strain tensor c_{ijkl} is reduced to a two-dimensional matrix **C**.

Using the element nodal values $\mathbf{d}^e$ and $\mathbf{p}^e$,

$$\boldsymbol{\varepsilon} = -\sum_{a=1}^{n_{en}^d} \mathbf{B}_a \mathbf{d}_a^e, \tag{20}$$

$$\varepsilon_v = -\sum_{a=1}^{n_{en}^d} \mathbf{b}_a^{\mathrm{T}} \mathbf{d}_a^e, \tag{21}$$

$$\mathbf{grad}\ \rho = \sum_{b=1}^{n_{en}^p} \mathbf{E}_b p_b^e, \tag{22}$$

where n_{en}^d and n_{en}^p are the number of element nodes interpolating **u** and ρ in the element domain Ω^e, respectively, ε_v is the volumetric strain, **grad** ρ is the n_{sd}-dimensional pressure gradient vector, and matrix $\mathbf{B}_a$ is the *strain-displacement* matrix. The negative signs for $\boldsymbol{\varepsilon}$ and ε_v are consistent with the definition for compressive strains being positive.

In three-dimensional analysis,

$$\mathbf{B}_a = \begin{bmatrix} B_1 & 0 & 0 \\ 0 & B_2 & 0 \\ 0 & 0 & B_3 \\ B_2 & B_1 & 0 \\ 0 & B_3 & B_2 \\ B_3 & 0 & B_1 \end{bmatrix}, \tag{23}$$

$$\mathbf{b}_a^{\mathrm{T}} = \{1, 1, 1, 0, 0, 0\} \cdot \mathbf{B}_a, \tag{24}$$

in which $B_i = \partial N_a / \partial x_i$, where N_a is the displacement shape function associated with node a, while

$$\mathbf{E}_b = \left[\frac{\partial \hat{N}_b}{\partial x_1}, \frac{\partial \hat{N}_b}{\partial x_2}, \frac{\partial \hat{N}_b}{\partial x_3}\right]^{\mathrm{T}}, \tag{25}$$

where $\hat{N}_b$ is the pressure shape function associated with pressure node b.

The global arrays **K**, **G**, $\mathbf{G}^{\mathrm{T}}$, **M**, $\dot{\mathbf{F}}$ and $\dot{\mathbf{H}}$ are then assembled from the following element contributions (cf. Table 1)†:

1. Element tangent stiffness matrix:

$$\mathbf{K}_{(n_{ed} \times n_{ed})}^e = \int_{\Omega^e} \mathbf{B}^{\mathrm{T}} \mathbf{C} \mathbf{B}\, d\Omega \tag{26}$$

where n_{ed} is the number of displacement components for element e (=number of displacement degrees of freedom per node × number of displacement nodes), and **C** is the rank-two stress-strain matrix obtained by contracting the indices of c_{ijkl}. The strain-displacement matrix **B** consists of nodal submatrices $\mathbf{B}_a = [\mathbf{B}_1, \mathbf{B}_2, \ldots, \mathbf{B}_{n_d}]$, where n_d is the number of element displacement nodes.

† Note sign reversals in all terms containing (compressive) stress rates $\{\dot{\sigma}^0\}$ and pressures ϱ and r.

2. Element coupling matrices:

$$\mathbf{G}^e_{(n_{ed}\times n_p)} = -\int_{\Omega^e} \mathbf{b}\hat{\mathbf{N}}^T \, d\Omega, \tag{27a}$$

$$(\mathbf{G}^e)^T_{(n_p\times n_{ed})} = -\int_{\Omega^e} \hat{\mathbf{N}}\mathbf{b}^T \, d\Omega, \tag{27b}$$

where n_p is the number of element pressure nodes and $\hat{\mathbf{N}} = \{\hat{N}_1, \hat{N}_2, \ldots, \hat{N}_{n_p}\}^T$ (see (17a, b)).

3. Element flux matrix:

$$\mathbf{M}^e_{(n_p\times n_p)} = -\frac{1}{\gamma_w}\int_{\Omega^e} \mathbf{E}^T\mathbf{k}\mathbf{E} \, d\Omega. \tag{28}$$

4. Element force vectors:

$$\dot{\mathbf{F}}^e_{(n_{ed}\times 1)} = \int_{\Omega^e} \mathbf{N}^T\dot{\mathbf{f}} \, d\Omega - \int_{\Omega^e} \mathbf{B}^T\dot{\sigma}^0 \, d\Omega + \int_{\Gamma^e_h} \mathbf{N}^T\dot{\mathbf{h}} \, d\Gamma - [\mathbf{K}^e\cdot\dot{\mathbf{d}}_g - \mathbf{G}^e\cdot\dot{\mathbf{p}}_r] \tag{29}$$

$$\dot{\mathbf{H}}^e_{(n_p\times 1)} = \int_{\Gamma^e_s} \hat{\mathbf{N}}^T s \, dT - [-(\mathbf{G}^e)^T\cdot\dot{\mathbf{d}}_g - \mathbf{M}\dot{\mathbf{p}}_r], \tag{30}$$

where $\mathbf{N}$ is an array consisting of element shape functions $\mathbf{N}_a$ such that $\mathbf{u} = \mathbf{N}\mathbf{d}$ (cf. (16a, b)); $\dot{\mathbf{d}}_g$ is an $(n_{ed}\times 1)$ vector containing prescribed g-displacements, i.e. $d_{g_i} = g_i$ if g_i is prescribed and $d_{g_i} = 0$, otherwise; $\mathbf{p}_r$ and $\dot{\mathbf{p}}_r$ are $(n_p\times 1)$ vectors containing prescribed r-pressures and pressure rates, respectively (similar definitions as for $\dot{\mathbf{d}}_g$).

2.5. *Time integration*

Suppose that the solution $(\mathbf{d}_n, \mathbf{p}_n)$ is known at time t_n, and that (18a, b) can be transformed into an incremental form in $(\Delta\mathbf{d}, \Delta\mathbf{p})$. A marching algorithm can then be employed to obtain the solution time t_{n+1}.

Integrating (18a, b),

$$\int_{t_n}^{t_{n+1}} \mathbf{K}\dot{\mathbf{d}} \, dt + \int_{t_n}^{t_{n+1}} \mathbf{G}\dot{\mathbf{p}} \, dt = \int_{t_n}^{t_{n+1}} \dot{\mathbf{F}} \, dt, \tag{31a}$$

$$\int_{t_n}^{t_{n+1}} \mathbf{G}^T\dot{\mathbf{d}} \, dt + \int_{t_n}^{t_{n+1}} \mathbf{M}\mathbf{p} \, dt = \int_{t_n}^{t_{n+1}} \dot{\mathbf{H}} \, dt, \tag{31b}$$

or

$$\bar{\mathbf{K}}\cdot\Delta\mathbf{d} + \mathbf{G}\cdot\Delta\mathbf{p} = \Delta\mathbf{F}, \tag{32a}$$

$$\mathbf{G}^T\cdot\Delta\mathbf{d} + \mathbf{M}\cdot\int_{t_n}^{t_{n+1}} \mathbf{p} \, dt = \Delta\mathbf{H}, \tag{32b}$$

where $\bar{\mathbf{K}}$ represents an *average value* of the tangent stiffness $\mathbf{K}$ over the time interval (t_n, t_{n+1}) (see, e.g. [9] for an evaluation of $\bar{\mathbf{K}}$ using a predictor-corrector algorithm). Factorization of the global matrices $\mathbf{G}$, $\mathbf{G}^T$, and $\mathbf{M}$ outside of the integral signs follows upon assumption that the permeability components of $\mathbf{k}$ do not change with time.

Equation (32b) may be transformed into a similar incremental form as (32a) using a discrete approximation to the remaining integral as follows:

$$\int_{t_n}^{t_{n+1}} \mathbf{p} \, dt \approx \Delta t[\beta\mathbf{p}_{n+1} + (1-\beta)\mathbf{p}_n] = \Delta t(\mathbf{p}_n + \beta\Delta\mathbf{p}). \tag{33}$$

An algorithm that uses $\beta = 0$ for the above approximation is called an *explicit Euler* algorithm. If $\beta = 1$, the algorithm is *purely implicit*. If $\beta = 1/2$, the approximation employs the *trapezoidal* or *midpoint* rule. The above approximation provides an unconditionally stable solution when $\beta \geqslant 1/2$[3] with optimum accuracy obtained when $\beta = 1/2$[4].

Using β as the integration parameter, a general incremental matrix equation is obtained, viz.

$$\begin{bmatrix} \bar{\mathbf{K}} & \mathbf{G} \\ \mathbf{G}^{\mathrm{T}} & \beta \Delta t \mathbf{M} \end{bmatrix} \begin{Bmatrix} \Delta \mathbf{d} \\ \Delta \mathbf{p} \end{Bmatrix} = \begin{Bmatrix} \Delta \mathbf{F} \\ \Delta \mathbf{H} - \Delta t \mathbf{M} \mathbf{p}_n \end{Bmatrix}, \tag{34}$$

where $\mathbf{p}_n$ is the nodal pore pressure vector at the start of the increment.

A similar incremental matrix equation of the form (34) has also been obtained by Small *et al.*[13] for the special case where $\mathbf{d}_g = 0$, $\mathbf{p}_r = 0$ and $\dot{\boldsymbol{\sigma}}^0 = 0$ using the principle of virtual work. The resulting system of simultaneous equations can be solved by any acceptably efficient numerical technique, say by Crout elimination[14].

3. NUMERICAL EXAMPLES

The following examples demonstrate the accuracy of the foregoing numerical procedure using a finite element program, called SPIN 2D, which employs the above integration scheme. The parameter β was set to 1/2, facilitating an unconditionally stable solution for any value of Δt. Quadrilateral elements were used with nine nodes (biquadratic Lagrangian) interpolating the displacement field, and four nodes (bilinear) interpolating the pore pressure field continuously across the element boundaries.† Standard Gaussian quadrature rules were employed in the numerical integration, i.e. 3×3 rule on element stiffness $\mathbf{K}^e$ and 2×2 rule on element matrices $\mathbf{G}^e$, $(\mathbf{G}^e)^{\mathrm{T}}$ and $\mathbf{M}^e$.

In examples 3.1–3.3 the soil skeleton was assumed to be isotropic, homogeneous and linearly elastic. In examples 3.1 and 3.2 Young's modulus $E = 7280$ and Poisson's ratio $\nu = 0.3$, giving a constrained modulus $E_c = 9800$ (consistent units are implied). In example 3.3, $\nu = 0.0$, $E = E_c = 10^4$.

3.1. *One-dimensional elastic consolidation*

Explicit solutions are available for problems involving consolidation in one dimension. The *average degree of consolidation* is given by[12]

$$\bar{U} = 1 - \frac{8}{\pi^2} \sum_{m=0}^{\infty} \frac{1}{(2m+1)^2} e^{-[\pi^2(2m+1)^2/4]T_v}, \tag{35}$$

where the time factor $T_v = c_v t / H^2$, in which c_v is the coefficient of consolidation, t is the natural time and H is half the distance between opposite drainage boundaries. The average degree of consolidation also gives the ratio between the current vertical settlement and the ultimate settlement at 100% pore pressure dissipation. A plot of $\bar{U}$ versus log T_v is shown in Fig. 2.

Letting $H = 1.0$ and $c_v = 1.0$, then $T_v = t$; assuming $\gamma_w = 9.8$, then the permeability $k = c_v \gamma_w / E_c = 0.001$.

The numerical results, obtained from the ratio of the current to ultimate settlements, are plotted in Fig. 2. Very good fit can be observed specifically at large values of T_v. The results for small T_v can be improved by subdividing Δt further into smaller increments.

3.2. *Radial elastic consolidation, free strain*

Explicit solutions are also available for the condition in which drainage goes radially, while allowing the loaded surface to deform so that the stress distribution on the soil remains constant. The average degree of consolidation for free-strain, radial drainage is

† See [4, 7, 10] on discontinuous pressure interpolation in incompressible applications.

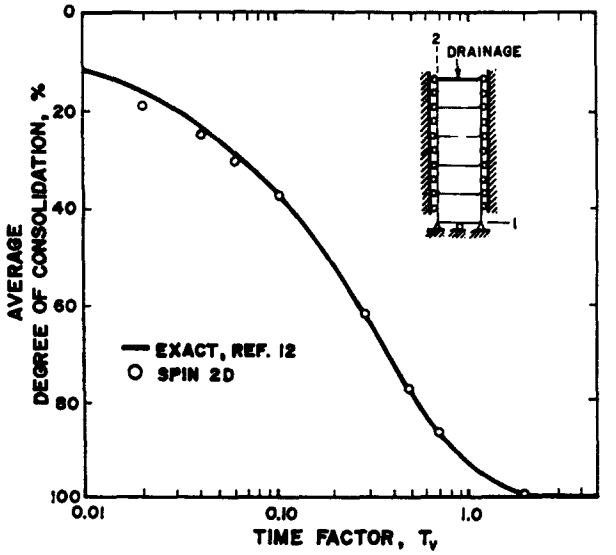

Fig. 2. One-dimensional consolidation.

given by[12]

$$\bar{U} = 1 - 4 \sum_{n=1}^{\infty} \frac{1}{\beta^2} e^{-\beta_n^2 T_v}, \tag{36}$$

where $\pm\beta$ are the roots of the equation $J_0(\beta) = 0$, in which J_0 is a Bessel function of the first kind and order zero. A plot of $\bar{U}$ versus T_v is shown in Fig. 3.

Letting the coefficient of radial consolidation $c_r = 1.0$ and radius $R = 1.0$ (see Fig. 3), the excess pore pressures were allowed to diffuse radially. The numerical results, obtained as the weighted average (by volume) of the dissipated pore pressure, are also plotted in Fig. 3. The same conclusion can be drawn as in example 3.1.

3.3. *Two-dimensional plane strain consolidation of an infinite elastic half-space*

A closed form solution is available for consolidation of an infinite elastic half-space subjected to a uniform strip load[6]. Figure 4 shows the problem geometry as represented by a mesh of 100 finite elements. In the following, $c_v = 1.0$, $\gamma_w = 9.8$, $k_{11} = k_{22} = c_v\gamma_w/E_c = 9.8 \times 10^{-4}$, $k_{12} = k_{21} = 0.0$.

Case a. *Strip load applied instantaneously.* Defining the dimensionless time factor $T = c_v t/B^2$, where B is half the width of the strip load, the load-time function for the

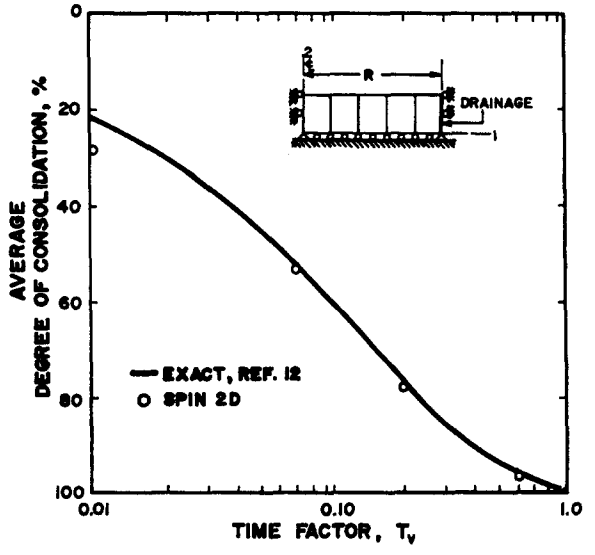

Fig. 3. Radial consolidation, free strain.

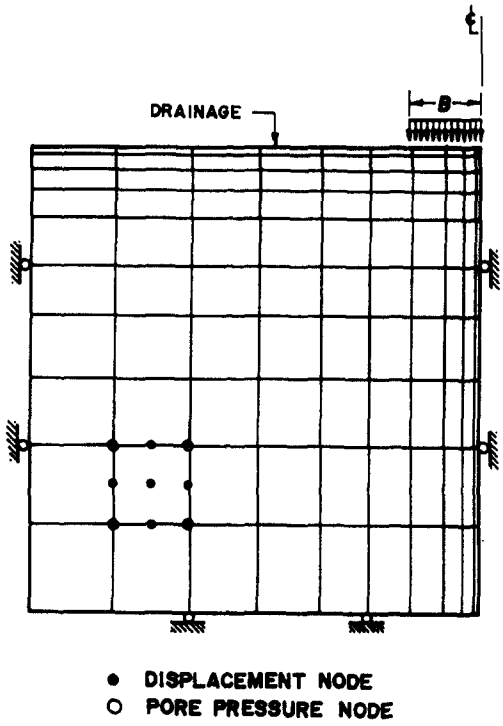

Fig. 4. Two-dimensional plain strain consolidation, problem geometry.

condition in which the load is applied instantaneously is a step function varying from zero at $T = 0.0$ to its full value p at $T = T_0 = 0^+$ (Fig. 5). A plot of the normalized centerline pore pressure at depth $z = 0.5B$ versus T is shown in Fig. 5.

Superimposed in Fig. 5 are the results of a numerical test consisting of 10 variable time steps, the first time step simulating a semiundrained condition in which $\Delta T = 10^{-10}$, generating an initial pore pressure $= 0.712p$ (exact $= 0.705p$ for the totally undrained case). Excellent agreement between the numerical and analytical results can be observed.

Case b. *Strip load applied gradually.* To investigate the influence of the rate of loading, two computer runs were made with the strip load attaining its full value p gradually with time. Assuming that the intensity of the strip load increases linearly with the time factor T,

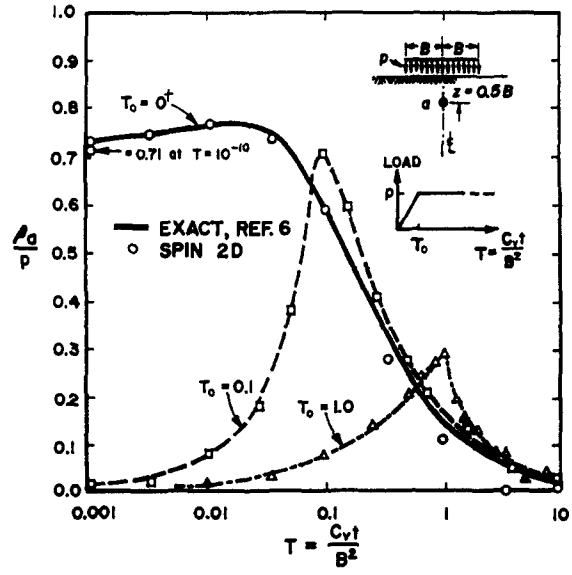

Fig. 5. Centerline pore pressure at depth $z = 0.5B$ beneath a strip load.

plots of excess pore pressures versus time for the cases in which $T_0 = 0.1$ and $T_0 = 1.0$ are shown in Fig. 5. Since no significant dissipation of excess pore pressures occurs until $T \approx 0.1$ in Case a, it can be concluded that the peak value of excess pore pressure at the centerline where $z = 0.5B$ can be markedly reduced if the strip load is applied gradually such that $T_0 > 0.1$.

4. SUMMARY AND CONCLUSION

The transient condition of pore pressure dissipation has been analyzed in this report by considering the two-phase soil–water structure of a saturated soil mass. The governing matrix equation for use in the finite element analysis has been derived using variational concepts involving coupled displacement and pore pressure fields. A family of trapezoidal integration, specified by the integration parameter β, was employed to facilitate the evolution of the solution with time. The accuracy of the above integration scheme has been demonstrated in one- and two-dimensional applications using a finite element program which employs the foregoing numerical procedure.

Acknowledgment—The author is most grateful to Professor T. J. R. Hughes of Stanford University for his helpful suggestions concerning both the theoretical formulation and numerical implementation of this work. Funding for this research was provided in part by a grant from the National Science Foundation.

REFERENCES

1. E. B. Becker, G. F. Carey and J. T. Oden, *Finite Elements, An Introduction*, Vol. 1. Prentice-Hall, Englewood Cliffs, New Jersey (1981).
2. M. A. Biot, General theory of three-dimensional consolidation. *J. Appl. Phys.* **12**, 155–164 (1941).
3. J. R. Booker and J. C. Small, An investigation of the stability of numerical solutions of Biot's equations of consolidation. *Int. J. Solids Structures* **11**, 907–917 (1975).
4. R. I. Borja, Finite element analysis of the time-dependent behavior of soft clays. Ph.D. thesis, Stanford University, Stanford, California (1984).
5. R. I. Borja and E. Kavazanjian, Jr., A constitutive model for the stress-strain-time behavior of "wet" clays. *Geotechnique* **35**(3) (1985).
6. A. T. F. Chen, Plane strain and axi-symmetric primary consolidation of saturated clays. Ph.D. thesis, Rensselaer Polytechnic Institute, Troy, New York (1966).
7. J. T. Christian, Two- and three-dimensional consolidation. In *Numerical Methods in Geotechnical Engineering* (Edited by C. S. Desai and J. T. Christian), Chap. 12, pp. 399–426. McGraw-Hill, New York (1977).
8. Y. C. Fung, *Foundations of Solid Mechanics*. Prentice-Hall, Englewood Cliffs, New Jersey (1965).
9. T. J. R. Hughes and J. H. Prévost, DIRT II—a nonlinear quasi-static finite element analysis program. User's manual (1979).
10. T. J. R. Hughes, Mixed and penalty methods, reduced and selective integration, and sundry variational crimes. In *A Course in the Finite Element Method*, Vol. 1, Chap. 4. Stanford University, preprint (1982).
11. L. E. Malvern, *Introduction to the Mechanics of a Continuous Medium*. Prentice-Hall, Englewood Cliffs, New Jersey (1969).
12. R. F. Scott, *Principles of Soil Mechanics*. Addison-Wesley, New York (1963).
13. J. C. Small, J. R. Booker and E. H. Davis, Elasto-plastic consolidation of soil, *Int. J. Solids Structures* **12**, 431–448 (1976).
14. R. L. Taylor, Computer procedures for finite element analysis. In *The Finite Element Method* (Edited by O. C. Zienkiewicz), 3rd edn, Chap. 24. McGraw-Hill, London (1977).